Icarus 210 (2010) 8–13

Contents lists available at ScienceDirect

Icarus

journal homepage: www.elsevier.com/locate/icarus

Deconvolution of lunar olivine reflectance spectra: Implications for remote compositional assessment

Peter J. Isaacson *, Carlé M. Pieters

Department of Geological Sciences, Brown University, Box 1846, RI 02912, United States

ARTICLE INFO

Article history:
Received 5 April 2010
Revised 8 June 2010
Accepted 9 June 2010
Available online 15 June 2010

Keywords:
Spectroscopy
Mineralogy
Data reduction techniques
Moon, Surface

ABSTRACT

Lunar olivines typically contain inclusions of Cr–spinel (chromite) that influence their measured optical properties. These altered optical properties complicate modeled predictions of olivine composition from reflectance spectra. Approaches developed for inclusion-free terrestrial olivine spectra must be modified to be applied to chromite-bearing lunar olivine spectra. We present a revised approach for predicting the compositions of chromite-bearing lunar olivines using the Modified Gaussian Model (MGM). The results of this revised approach for chromite-bearing lunar olivines are consistent with previous results for terrestrial olivine reflectance spectra, and successfully predict the olivine's composition. These results are an important step in compositional assessment of remotely-sensed olivine spectra, and are essential to ongoing investigations of that topic. Our results are based on a limited set of available lunar olivine separates, and would be strengthened by the inclusion of additional compositions.

1. Introduction

The thermal and chemical evolution of planetary bodies is a major guiding theme in planetary science and exploration. Planetary bodies cool in a number of ways, including magma ocean processes, density stratification (differentiation), internal convection, and volcanism. These processes affect the chemical evolution of planetary bodies, as the composition and mineralogy of zones within the bodies evolve as thermal evolution progresses. Rocks contain distinct records of the thermal history of a planetary body, as their mineralogy and mineral composition are products of the processes that produced and/or altered them. Olivine in particular is a very important mineral with which to interpret the petrologic evolution of igneous rocks, as it is commonly the first mineral to crystallize from typical mafic magmas (BVSP, 1981). In the case of a primary magma, the olivine's composition indicates the degree of evolution of the mantle source of the magma from which the olivine crystallized. Generally speaking, highly forsteritic (high Mg′ (Mg/Mg + Fe)) olivine is indicative of a primitive source, whereas more fayalitic (low Mg′) olivine is indicative of a more evolved source (BVSP, 1981). The composition of lunar olivine is an indicator used to determine if a rock is from a particular lithologic suite (Hess, 1994; Papike et al., 1998; Warner et al., 1976; Warren and Wasson, 1977).

Olivine has a distinctive signature in visible to near-infrared (VNIR) reflectance spectra. Typical olivine spectra have a broad, composite absorption feature near 1050 nm caused by electronic transitions in Fe^{2+} ions located in distorted octahedral crystal lattice sites (Burns, 1970, 1974, 1993; Burns et al., 1972). An example is illustrated in Fig. 1, which shows a spectrum of San Carlos olivine ($\sim Fo_{90}$), a common laboratory standard sample. The three absorptions that comprise the composite feature are labeled with the Fe^{2+}-bearing crystallographic site responsible for the specific absorption. Visible to near-infrared reflectance spectroscopy is sensitive to olivine composition, because these three absorption features shift as a function of the olivine's Mg′ (Burns, 1970; King and Ridley, 1987; Sunshine and Pieters, 1998). When individual absorption bands are deconvolved with quantitative techniques such as the Modified Gaussian Model (MGM) (Sunshine et al., 1990), olivine reflectance spectra can be used to estimate the olivine's composition by inverting the MGM-derived band parameters to solve for composition as a function of band position (Sunshine and Pieters, 1998).

Reflectance spectra of typical lunar olivines differ from those of terrestrial and synthetic olivine (Isaacson and Pieters, 2008; Isaacson et al., 2010). Lunar olivines often contain small but significant abundances of fine Cr–spinel inclusions (e.g., Dymek et al., 1975; Papike et al., 1998). Spinels have strong absorption features beyond ~1600 nm (Cloutis et al., 2004), a wavelength region where typical terrestrial olivines are bright and featureless. A laboratory reflectance spectrum of a typical Cr–spinel (chromite) is shown in Fig. 1. Olivine is a relatively transparent mineral, therefore strongly absorbing opaque inclusions, such as spinels, have

* Corresponding author. Fax: +1 401 863 3978.
E-mail addresses: Peter_Isaacson@Brown.edu (P.J. Isaacson), Carle_Pieters@Brown.edu (C.M. Pieters).

0019-1035/$ - see front matter © 2010 Elsevier Inc. All rights reserved.
doi:10.1016/j.icarus.2010.06.004

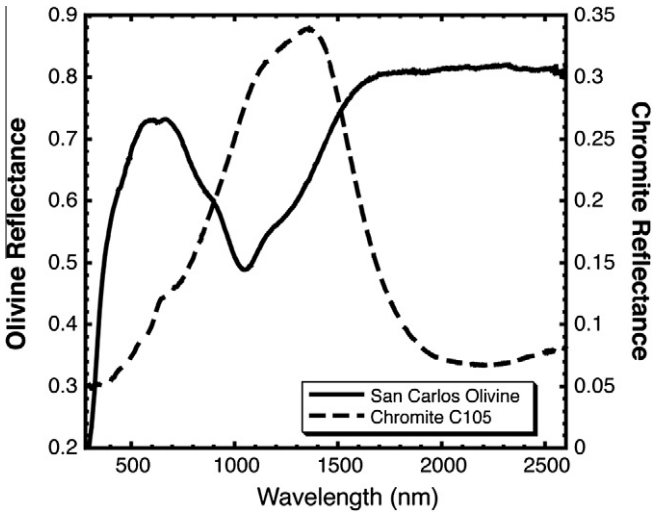

Fig. 1. Bidirectional reflectance spectra of terrestrial olivine and chromite. San Carlos olivine (~Fo_{90}) is labeled with the specific Fe^{2+}-bearing site causing each of the component absorptions. The chromite spectrum is described by Cloutis et al. (2004), sample C105.

dramatic effects on olivine reflectance spectra, even in trace amounts. Chromite-bearing lunar olivine spectra are not featureless beyond the principal composite crystal-field ferrous absorption (wavelengths above ~1500 nm). Instead, chromite-bearing lunar olivine spectra drop in reflectance across this region due to the chromite inclusions. The differences between chromite-bearing lunar olivine and terrestrial olivine spectra have significant, adverse effects on the deconvolution of the spectra with approaches such as the MGM. The presence of the strong long-wavelength absorptions in lunar olivine spectra requires the inclusion of absorptions in the model that interfere with fits to the primary olivine ferrous crystal-field absorptions. The result of these complications is that the standard approach developed for spectra of terrestrial olivine (Sunshine and Pieters, 1998) is unable to estimate the composition of lunar olivine samples with any accuracy (Isaacson and Pieters, 2008). A revised, systematic approach for chromite-bearing lunar olivine is required if the richness of information available from global analyses of remotely-sensed spectra of lunar olivine is to be harvested. The arrival of global hyperspectral lunar datasets (Mall et al., 2009; Matsunaga et al., 1999; Pieters et al., 2009) collected by Kaguya and Chandrayaan-1 is now enabling such remote compositional analyses, making this revised approach an important element of ongoing research of lunar olivine composition through remote sensing.

2. Background: MGM fits of olivine spectra

2.1. Traditional approach

The MGM is an inverse model that allows the user to deconvolve a spectrum into a set of absorptions superimposed onto a continuum slope. Mathematically, the absorptions are defined by Gaussian distributions in average bond length of the site and cation of interest, and in the model are expressed as three parameters for each absorption: band center, band width, and band strength. The continuum slope is defined by a set of polynomial coefficients, which act as additional model parameters. The model adjusts the various models parameters to minimize, in a least squares sense, the sum of the squares of the residuals. It is important to remember that models such as the MGM seek to minimize the error of a fit without regard for whether the resulting model parameters are consistent with the structure of the mineral or mixture in question. The reader is referred to the work of Sunshine et al. (1990) for additional background on the MGM, approach, and underlying mathematics. For laboratory spectra of terrestrial olivines, a flat continuum slope is commonly used, and the offset (*y* intercept value) of the continuum is allowed to vary freely in the optimization routine. The MGM initial parameters are defined by three absorptions near 1000 nm for the principal olivine feature, and two absorptions at shorter wavelengths to account for absorptions in the visible to near-ultraviolet. The result of such a fit performed on the San Carlos olivine spectrum shown in Fig. 1 is illustrated in Fig. 2a. MGM results for this and all other fits shown or described in this paper are provided in Table 1. Intensities are reported as natural log reflectance, whereas band centers and

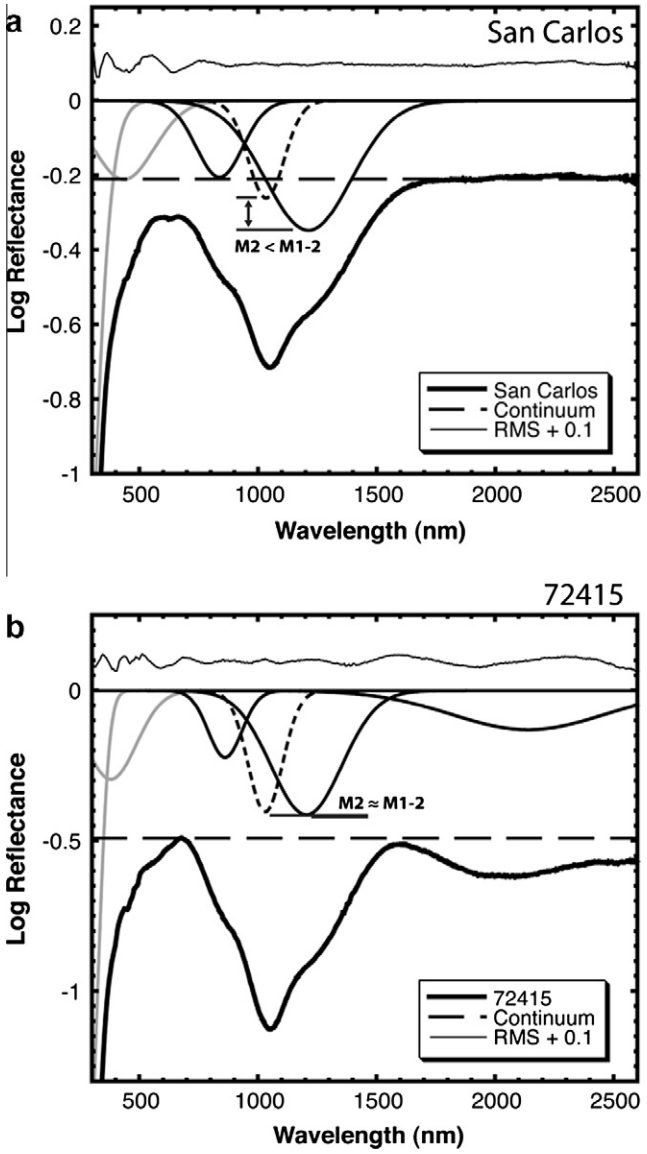

Fig. 2. Example MGM fits to olivine spectra using the standard approach described by Sunshine and Pieters (1998). (a) Fit to San Carlos olivine (~Fo_{90}) spectrum shown in Fig. 1. This is an example of a high-quality fit. (b) Fit to spectrum of lunar olivine separated from 72415 (~Fo_{88}). The effect of the chromite inclusions is seen in the reduced reflectance and the absorption feature beyond 1500 nm. Even when adding an absorption to account for the chromite absorption, an unsatisfactory fit is produced, as evidenced by the RMS error and inconsistent band properties of the three olivine absorptions as compared to the San Carlos olivine fit in (a). The relative band strengths between the M2 and M1-2 absorptions are highlighted, showing the similar modeled strengths for the M2 and M1-2 absorptions in (b).

Table 1
Results of MGM fits.

Fo#	Info	Figure	M1-1, center	M1-1, FWHM	M1-1, intensity	M2, center	M2, FWHM	M2, intensity	M1-2, center	M1-2, FWHM	M1-2, intensity	Fo# pred.
90	San Carlos	2a	836.1	231.1	−0.2042	1032.3	178.4	−0.2602	1210.8	426.1	−0.3471	91.5
88	72415	2b	859.9	167.7	−0.2212	1029.5	170.6	−0.4024	1203.0	350.2	−0.4126	85.7
88	72415 Mg-rich	4, 5	844.1	227.9	−0.3707	1036.7	180.3	−0.4456	1218.3	321.5	−0.6585	82.9
88	72415 Int.	3a, 4, 5	844.1	227.9	−0.3706	1036.7	180.3	−0.4455	1218.2	457.5	−0.6585	83.0
88	72415 Fe-rich	4, 5	843.2	227.5	−0.3462	1036.9	175.7	−0.4127	1209.4	478.6	−0.6659	88.0
87	76535 Mg-rich	4, 5	848.9	229.7	−0.4903	1035.3	185.7	−0.4954	1223.1	460.8	−0.7733	78.6
87	76535 Int.	3b, 4, 5	848.9	229.7	−0.4902	1035.3	185.7	−0.4953	1223.1	460.8	−0.7733	78.6
87	76535 Fe-rich	4, 5	849.0	229.2	−0.4671	1035.3	180.7	−0.4599	1215.1	479.2	−0.7814	82.8
48	15555 Mg-rich	4, 5	869.9	234.3	−0.981	1045.0	202.3	−0.7459	1255.3	501.5	−1.4066	49.6
48	15555 Int.	3c, 4, 5	869.8	234.3	−0.981	1045.0	202.5	−0.7469	1255.4	501.3	−1.4065	49.6
48	15555 Fe-rich	4, 5	870.9	233.6	−0.9483	1045.5	197.2	−0.6926	1249.2	520.0	−1.4162	52.2

widths (FWHM) are reported in nanometers (nm). As expected, the model parameters derived from this fit (absorption band center, width, and strength) are consistent with the trends derived by Sunshine and Pieters (1998). The RMS error across the visible wavelengths does not affect the critical 1000 nm region of the fit, and is a result of simplifying the fit across this region.

2.2. Inadequacy of traditional approach for lunar olivine spectra

Also illustrated in Fig. 2b is an example result from applying the approach described above to a spectrum of chromite-bearing lunar olivine. The lunar olivine sample illustrated in Fig. 2b (separated from dunite sample 72415) is very similar in Mg′ to the San Carlos olivine illustrated in Fig. 2a (Fo_{88} for 72415, Fo_{90} for San Carlos). Thus, the band centers and band widths of the three principal absorption features should be nearly identical between the spectra. Absolute band strength varies as a function of grain size and other textural properties of a sample, although relative band strengths should be similar. The prominent absorption near 2000 nm in these olivine spectra is attributed to the chromite inclusions, and an additional absorption is added to account for this feature. The modeled fit plotted in Fig. 2b is unrealistic for many reasons, including the RMS error, relative band positions, and relative band strengths. Specifically, the band positions are inconsistent with results for the San Carlos olivine, especially for the M1-1 band, and the central M2 absorption is modeled with similar strength to the M1-2 absorption, as illustrated by Fig. 2b. This similarity in band strength between M2 and M1-2 is inconsistent with previous analyses of olivine spectra (Burns, 1970; Sunshine and Pieters, 1998). Clearly, the standard approach developed for terrestrial samples returns substantially different results when applied to spectra of chromite-bearing lunar olivines, even when an additional band is included in the fit in an attempt to account for the spinel feature.

The poor fit is caused primarily by two factors, both related to the spinel absorptions: the spinel absorption severely reduces the overall reflectance at long wavelengths (>1500 nm) and also introduces another feature that the model attempts to include in minimizing the error in the fit. The traditional approach relies on a bright, flat region beyond 1500 nm on which the flat continuum slope is based (the fit in Fig. 2a is an excellent example, as the reflectance at wavelengths >1500 nm is much higher than the reflectance maximum at wavelengths below the 1000 nm absorption feature, near ~700 nm). The spectrum in Fig. 2b has nearly identical maximum reflectance values at wavelengths above and below the 1000 nm absorption, so a flat continuum slope cannot come to rest on a high value as in Fig. 2a. The continuum slope intersects the spectrum in Fig. 2b, which creates problems when fitting the first M1 olivine absorption in particular. Additionally, the absorption added to account for the spinel feature expands to such extreme widths that it expands into the 1000 nm region, and interferes with the fit in this critical wavelength region. Generally, this approach does not produce acceptable results for lunar olivine reflectance spectra.

3. Revised MGM approach for lunar olivine

MGM deconvolutions of remotely-sensed lunar olivine spectra will be complicated largely by two factors: the chromite absorptions discussed above, and the variable continuum slopes common to remotely-sensed spectra of planetary surfaces. The original approach developed by Sunshine and Pieters (1998) and the revised approach presented here rely on flat continuum slopes, which are likely to be unrealistic for remotely-sensed spectra. This paper addresses the complications resulting from chromite absorptions. Treatment of complications due to continuum slope is the focus of ongoing work. Note that the approach described here is applicable to any lunar olivine reflectance spectrum, regardless of the presence of absorptions caused by chromite inclusions. Thus, this technique can be applied safely without requiring the user to make a subjective evaluation of the presence of long-wavelength chromite absorptions.

3.1. Wavelength range

We have revised the deconvolution approach outlined above to account for the complications due to chromite absorptions in laboratory spectra of lunar olivines. The modification includes two fundamental steps: truncate the spectrum and enforce a flat continuum slope. In this approach, spectra of lunar olivines are fit between wavelengths of 600 and 1750 nm. Wavelengths shorter than 600 nm do not contribute to the compositional analysis method

discussed here. The 600 nm cutoff was chosen to allow full modeling of the first M1 olivine band; a longer cutoff wavelength would run the risk of eliminating some data needed to constrain that band fully. The 1750 nm cutoff was chosen as a compromise between avoiding the bulk of the spinel feature and fully capturing the long-wavelength M1 olivine band. In addition to the three principal olivine absorptions, two additional absorptions are included in the revised modeling approach to account for the residual spectral structure at short and long wavelengths. Note that this approach addresses the dominant source of error (the long-wavelength chromite absorptions) in applying the traditional deconvolution approach to chromite-bearing lunar olivine spectra, but does not address the more minor effect of the reflectance maximum in the chromite spectra that occurs near the olivine M1-2 absorption.

3.2. Continuum slope

The choice of continuum slope has significant effects on band strength and width as well as band position, and systematic results rely on a systematic selection of continuum slope. For consistency, we use flat continuum slopes, which are appropriate for laboratory spectra. The flat continuum slope can be modeled with a variety of offset values. We have experimented with a variety of offsets, and have found that increasing the offset value such that the initial continuum slope lies well above the spectrum being deconvolved produces results most consistent with the terrestrial trends. If the initial continuum slope has an offset value that is too low, the three principal absorptions are not given enough freedom to "move" and do not converge on physically reasonable results. In an extreme case, the continuum slope can even intersect the spectrum, producing especially poor results. In our experience, it is better to err on the side of a continuum offset that is too large rather than too small. The chosen offset will affect the absolute strengths of the absorption features, but will not affect the relative band strengths. However, excessive offset values could introduce errors by allowing broadening of the two additional bands included with the three principal olivine absorptions in the model fits.

The results of applying this revised MGM approach for lunar olivine are illustrated in Fig. 3. The three principal olivine absorptions are plotted in black, and the two additional absorptions discussed above are plotted in gray. The three lunar olivine spectra evaluated and plotted in Fig. 3 are: 72415 (~Fo_{88}), Fig. 3a; 76535 (~Fo_{87}), Fig. 3b; 15555 (~Fo_{48}), Fig. 3c. All lunar olivines were measured with a particle size of <125 μm. While band centers are the principal basis of the compositional assessment, a fit is not considered satisfactory if the relative band strengths of the three olivine absorptions are not consistent with known trends (Burns, 1970; Sunshine and Pieters, 1998). The results in Fig. 3 suggest that the modifications introduced to deal with the long-wavelength spinel absorptions are functioning appropriately.

3.3. Model initial conditions

Three distinct starting points were tested for MGM deconvolutions of the lunar olivine spectra. Reasonable model parameters for Mg-rich (~Fo_{90}), Fe-rich (~Fo_{45}) and intermediate (~Fo_{70}) compositions were chosen based on the Sunshine and Pieters (1998) results. This approach was taken to evaluate the sensitivity of the approach to the initial model parameters in the ideal case of laboratory spectra and to optimize the starting conditions for our fits. This is an important consideration, because the nonlinear MGM must be given a reasonable starting point. Model parameters for our three starting conditions are provided in Table 2. As in Table 1,

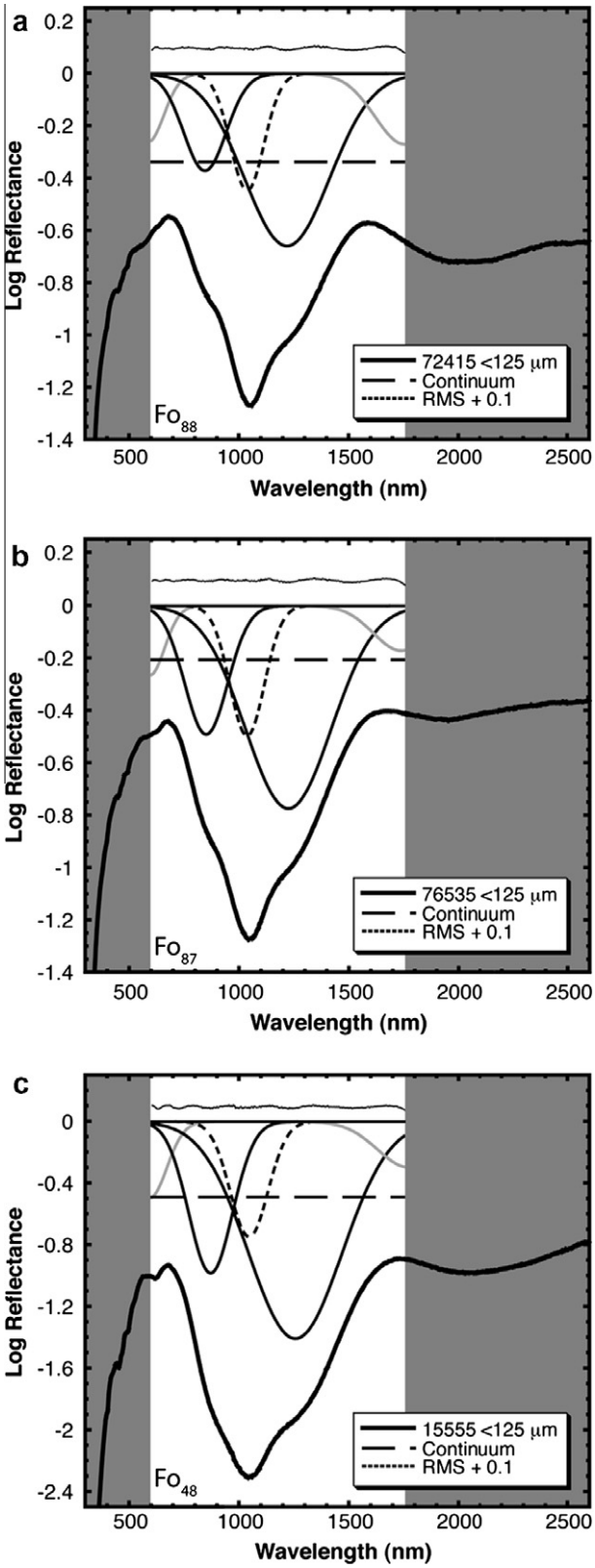

Fig. 3. Revised approach for MGM deconvolution of chromite-bearing lunar olivine reflectance spectra. Gray areas indicate wavelengths excluded from MGM deconvolutions in our approach. The three lunar olivine spectra analyzed in this study are shown with example MGM fits using our approach. All olivine spectra illustrated in this figure were measured with a particle size of <125 μm: (a) 72415 (~Fo_{88}); (b) 76535 (~Fo_{87}); (c) 15555 (~Fo_{48}). The intermediate starting conditions (see Section 3.3) were used to produce the fits plotted here.

Table 2
MGM starting parameters.

Starting fit	Mg-rich ($\sim Fo_{90}$)	Intermediate ($\sim Fo_{70}$)	Fe-rich ($\sim Fo_{45}$)
Band, parameter			
Short, center	630	630	630
Short, width	115	115	115
Short, intensity	−0.02	−0.02	−0.02
M1-1, center	840	855	880
M1-1, width	228	228	228
M1-1, intensity	−0.2	−0.2	−0.2
M2, center	1036	1038	1055
M2, width	176	176	176
M2, intensity	−0.225	−0.225	−0.225
M1-2, center	1210	1232	1255
M1-2, width	424	424	460
M1-2, intensity	−0.275	−0.275	−0.275
Long, center	1650	1650	1650
Long, width	250	250	250
Long, intensity	−0.0125	−0.0125	−0.0125
Continuum offset (C0)	Variable	Variable	Variable
Continuum slope (C1)	1E−10	1E−10	1E−10

intensities are given in natural log reflectance, and band centers and widths (FWHM) are given in nanometers (nm). The results in Table 1 are coded (in shades of gray) according to the various initial conditions.

4. Results: consistency with compositional trends

Shown in Fig. 4 are the compositions of lunar olivines analyzed in this study plotted against the MGM-derived actual band centers (range brackets) and compared with the results of Sunshine and Pieters (1998) (open symbols) and the trends derived by the Sunshine and Pieters (1998) study of terrestrial olivine (dotted lines). The range brackets indicate the spread in band centers obtained from the different starting points for the MGM fits. In viewing the MGM results in Table 1, it is apparent that the Fe-rich starting point actually produces the most Mg-rich compositional predictions, especially for 72415. This is most easily seen by comparing the predicted Fo# from the three initial conditions applied to each spectrum. This is likely a result of the higher initial band width for

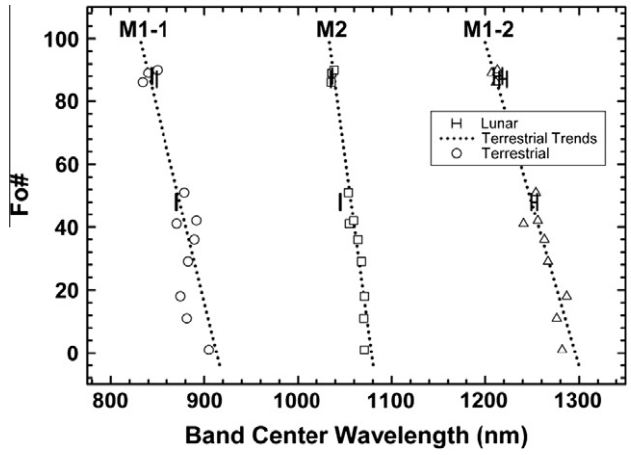

Fig. 4. Results of MGM deconvolutions of lunar olivine reflectance spectra as compared to results from Sunshine and Pieters (1998) for terrestrial olivine spectra. The actual Fo# of the olivines studied is plotted against the MGM-derived band centers. Range brackets represent the range of band center results produced from the three different starting points. Specific absorptions are labeled (M1-1, M2, M1-2). The MGM deconvolutions plotted here were derived from the "intermediate" starting conditions discussed in Section 3.3 and provided in Table 2. The MGM-derived parameters are provided in Table 1.

the M1-2 band in this starting condition, giving this fit slightly more freedom and producing a more Mg-rich result, which is more consistent with the actual olivine composition. The result for the Fe-rich starting point applied to the 15555 olivine is nearly identical to results derived from the other starting points for this spectrum, and all converge to reasonable parameters for this olivine's composition ($\sim Fo_{48}$).

The trends in lunar olivine band centers are reasonably consistent with those determined for terrestrial olivines by Sunshine and Pieters (1998). Based on the small sample size of the dataset (effectively two compositions of olivine), any assessment of systematic deviations from previously-established trends must be regarded with some amount of skepticism. Generally, it appears that fits to the basalt olivine spectrum ($\sim Fo_{48}$) produce band centers for the M2 absorption that are offset to short wavelengths relative to the Sunshine and Pieters (1998) results. However, the deviation from the trend lines is not substantially larger than observed in some of the scatter in the Sunshine and Pieters (1998) results. Further analysis of deviations between results of the revised approach for lunar olivine and the results for terrestrial olivine spectra (Sunshine and Pieters, 1998) will require more data points for lunar olivine (i.e., additional lunar olivine compositions) such that a true regression can be performed rather than fitting a two point line. The consistency between our results and the terrestrial trends suggests that a similar approach to compositional prediction as that employed for terrestrial olivine spectra may be employed for lunar olivine spectra. However, the robustness of the compositional predictions would be improved by complementing our work with additional lunar olivine compositions.

5. Discussion: compositional predictions from lunar olivine reflectance spectra

MGM deconvolutions of olivine spectra can be used to predict the composition of the olivine based on the trends in band positions previously established. We demonstrate with our approach that the trends in band centers for lunar olivine spectra are consistent with those demonstrated for terrestrial olivine spectra. However, these lunar trends are based on only a few data points, so we chose to use the trends developed from the suite of terrestrial olivines to evaluate the robustness of our results for compositional prediction. The use of the terrestrial olivine trend lines is acceptable because our deconvolution approach for lunar olivine provides results consistent with results for deconvolutions of terrestrial olivines with the traditional approach. We evaluate our results by treating our lunar olivine spectra as "unknowns" and predicting their composition from the fit results.

The compositional prediction method is based on minimization of the deviations in band centers from the established trends for all three absorption features simultaneously. Trend line equations are defined for each individual absorption band, and the unknown (Fo#) is parameterized in terms of the band center wavelength for each individual absorption (each linear trend line is defined by band center as a function of Fo#). The deviation of the band center wavelengths from the trend lines for each absorption is minimized by varying the Fo#. This process can be visualized by considering the deconvolution results as three points fixed in wavelength. These points are moved concurrently along the y axis in Fig. 4 (Fo# is varied) until the deviation between these points and the trend lines is minimized. The Fo# giving the minimum deviation from the three trend lines simultaneously is the predicted composition. This approach minimizes the effect of a deviation of a single absorption from the trends by weighting all three absorptions equally.

Fig. 5 demonstrates the results of "predicting" the composition for our lunar olivine spectra, as it plots the range of "predicted"

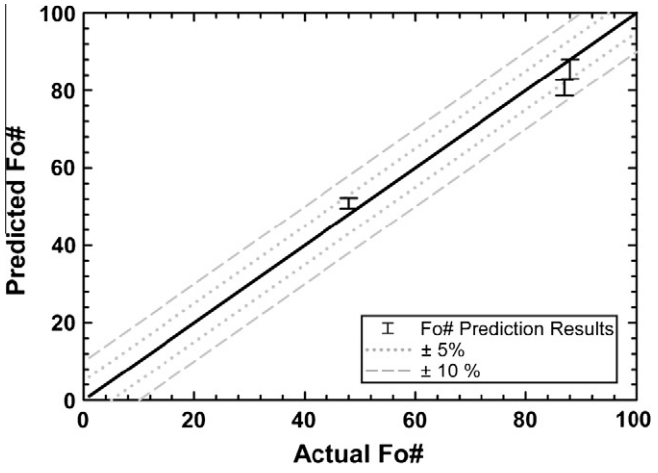

Fig. 5. Predicted Fo# vs. actual Fo# for lunar olivine spectra. Predicted Fo#'s are the result of treating the lunar olivines as unknowns, and "predicting" their compositions using the method outlined in the text. Range brackets illustrate the range of predicted compositions from the three starting points. These predictions should be considered a "best case scenario" for compositional predictions from lunar olivine reflectance spectra, and are accurate to within 5–10%.

composition when treating the spectrum as an unknown against the actual composition determined by independent elemental analysis techniques. The range in predicted compositions reflects the range in band centers resulting from the varied model starting points. The results generally fall within a range of 5–10% (5–10 Fo# range), indicating a very good accuracy of the predictions. Additionally, because we have used the trends derived for terrestrial olivine spectra to "predict" the composition of lunar olivines deconvolved with our revised approach, the very good agreement between predicted and measured compositions demonstrates both the accuracy of the prediction method for lunar olivine spectra and the consistency between results for the fitting procedures devised for lunar and terrestrial olivine spectra.

6. Conclusions

The common chromite inclusions in lunar olivines have dramatic effects on the reflectance spectra of lunar olivines between 1600 and 2600 nm. Approaches to deconvolving olivine spectra developed for terrestrial olivines are based on a full wavelength range (<600 nm to 2600 nm) and do not produce satisfactory results for lunar olivines. A new method for deconvolving lunar olivine spectra based solely on the reflectance between 600 and 1750 nm is successful at reproducing the expected trends in individual absorption band position. Because these trends are the basis of predicting the composition of an "unknown" olivine measured with reflectance spectroscopy, this revised approach for chromite-bearing lunar olivine spectra is a vital component of predictions of lunar olivine composition from remotely-sensed spectra.

Acknowledgments

The lunar olivine spectra analyzed in this study were measured in the RELAB at Brown University. The NASA RELAB is supported as a multi-user facility under Grant NNG06GJ31G. The authors gratefully acknowledge the support of NASA Grants NNM05AB26C and NNA09DB34A. Constructive reviews by Paul Lucey and Sarah Noble improved the quality of this manuscript substantially, and are greatly appreciated.

References

Burns, R.G., 1970. Crystal field spectra and evidence of cation ordering in olivine minerals. Am. Mineral. 55, 1608–1632.
Burns, R.G., 1974. The polarized spectra of iron in silicates: Olivine. A discussion of neglected contributions from Fe^{2+} ions in M(1) sites. Am. Mineral. 59, 625–629.
Burns, R.G., 1993. Mineralogical Applications of Crystal Field Theory. Cambridge University Press, New York.
Burns, R.G., Huggins, F.E., Abu-Eid, R.M., 1972. Polarized absorption spectra of single crystals of lunar pyroxenes and olivines. Moon 4, 93–102.
Basaltic Volcanism Study Project, 1981. Basaltic Volcanism on the Terrestrial Planets. Pergamon Press, Inc., New York.
Cloutis, E.A., Sunshine, J.M., Morris, R.V., 2004. Spectral reflectance-compositional properties of spinels and chromites: Implications for planetary remote sensing and geothermometry. Meteor. Planet. Sci. 39, 545–565.
Dymek, R.F., Albee, A.L., Chodos, A.A., 1975. Comparative petrology of lunar cumulate rocks of possible primary origin – Dunite 72415, troctolite 76535, norite 78235, and anorthosite 62237. Proc. Lunar Sci. Conf. 6, 301–341.
Hess, P.C., 1994. Petrogenesis of lunar troctolites. J. Geophys. Res. 99, 19083–19093.
Isaacson, P.J., Pieters, C.M., 2008. Detecting a broader lunar magnesian suite with orbital spectroscopy. Lunar Planet. Sci. 39, 1783.
Isaacson, P.J., Basu Sarbadhikari, A., Pieters, C.M., Klima, R.L., Hiroi, T., Liu, Y., Taylor, L.A., 2010. The lunar rock and mineral characterization consortium: Deconstruction and integrated analyses of mare basalts. Meteor. Planet. Sci., submitted for publication.
King, T.V.V., Ridley, W.I., 1987. Relation of the spectroscopic reflectance of olivine to mineral chemistry and some remote sensing implications. J. Geophys. Res. E: Planets 92, 11457–11469.
Mall, U., Banaskiewicz, M., Bronstad, K., McKenna-Lawlor, S., Nathues, A., Soraas, F., Vilenius, E., Ullaland, K., 2009. Near infrared spectrometer SIR-2 on Chandrayaan-1. Curr. Sci. 96, 506–511.
Matsunaga, T., Ohtake, M., Haruyama, J., Otake, H., 1999. A visible and near infrared spectrometer for Selenological and Engineering Explorer (SELENE): Performance and calibration requirements from scientific objectives. J. Remote Sens. Soc. Jpn. 19, 490–507.
Papike, J.J., Ryder, G., Shearer, C.K., 1998. Lunar samples. In: Papike, J.J. (Ed.), Planetary Materials. Mineralogical Society of America, Washington, DC, pp. 5.1–5.234.
Pieters, C.M., and 19 colleagues, 2009. The Moon Mineralogy Mapper (M3) on Chandrayaan-1. Curr. Sci. 96, 500–505.
Sunshine, J.M., Pieters, C.M., 1998. Determining the composition of olivine from reflectance spectroscopy. J. Geophys. Res. 103, 13675–13688.
Sunshine, J.M., Pieters, C.M., Pratt, S.F., 1990. Deconvolution of mineral absorption bands: An improved approach. J. Geophys. Res. 95, 6955–6966.
Warner, J.L., Simonds, C.H., Phinney, W.C., 1976. Genetic distinction between anorthosites and Mg-rich plutonic rocks: New data from 76255. Proc. Lunar Sci. Conf. 7, 915–917.
Warren, P.H., Wasson, J.T., 1977. Pristine nonmare rocks and the nature of the lunar crust. Proc. Lunar Sci. Conf. 8, 2215–2235.